

# In<sub>0.75</sub>Ga<sub>0.25</sub>As on GaAs submicron rings and their application for coherent nanoelectronic devices

Franco Carillo <sup>a,1</sup>, Giorgio Biasiol <sup>b</sup>, Diego Frustaglia <sup>a</sup>,  
Francesco Giazotto <sup>a</sup>, Lucia Sorba <sup>c</sup>, and Fabio Beltram <sup>a</sup>

<sup>a</sup>*NEST-INFM and Scuola Normale Superiore, I-56126 Pisa, Italy*

<sup>b</sup>*NEST-INFM and Laboratorio Nazionale TASC-INFM-CNR, Area Science Park,  
I-34012 Trieste, Italy*

<sup>c</sup>*NEST-INFM and Laboratorio Nazionale TASC-INFM-CNR, AREA Science  
Park, I-34012 Trieste, Italy and Università di Modena e Reggio Emilia, I-41100  
Modena, Italy*

---

## Abstract

Electron-phase modulation in magnetic and electric fields will be presented in In<sub>0.75</sub>Ga<sub>0.25</sub>As Aharonov-Bohm (AB) rings. The zero Schottky barrier of this material made it possible to nanofabricate devices with radii down to below 200 nm without carrier depletion. We shall present a fabrication scheme based on wet and dry etching that yielded excellent reproducibility, very high contrast of the oscillations and good electrical gating. The operation of these structures is compatible with closed-cycle refrigeration and suggests that this process can yield coherent electronic circuits that do not require cryogenic liquids. The InGaAs/AlInAs heterostructure was grown by MBE on a GaAs substrate [1], and in light of the large effective g-factor and the absence of the Schottky barrier is a material system of interest for the investigation of spin-related effects [2,3,4] and the realization of hybrid superconductor/semiconductor devices [5].

*Key words:* Aharonov-Bohm rings, mesoscopic transport, two-dimensional electron gas

*PACS:* 73.23.Ad, 73.63.-b, 75.47.Jn

---



---

<sup>1</sup> Corresponding author. E-mail: franco.carillo@sns.it

## 1 Introduction

In the framework of conventional electronics, the requirement of an increasing number of devices per unit area has been the leading motivation for progressive device shrinking. As far as coherent electronics is concerned device shrinking is desirable in order to enhance performance and to rise the maximum working temperature. Established technologies for defining nanostructures in two-dimensional electron gases (2DEGs) are: nano gates, atomic force microscopy lithography (AFML) [6] and etched side-walls. The first two techniques were successfully employed in GaAs/AlGaAs-based nanostructures [7]. Etched nanostructures, despite the strong confinement, have charge depletion layers at the border, the extension of which depends on the type of semiconductor. In the case of GaAs-based 2DEG depletion severely limits the smallest size of a device, being in this case larger than those obtainable using AFML. We want to demonstrate that the use of InGaAs based 2DEGs overcome this limit allowing to pattern nanostructures defined by etched side walls down to 80 nm line-width providing at the same time a good electric gating.

## 2 Device description and fabrication process

The heterostructure employed in this work was grown by MBE on a GaAs (100)-oriented substrate [1]. A sequence of  $\text{In}_x\text{Al}_{1-x}\text{As}$  layers of increasing In content was first deposited in order to ensure lattice matching with the upstanding 10 nm layer of  $\text{In}_{0.75}\text{Ga}_{0.25}\text{As}$  forming the quantum well. A 10-nm-thick  $\text{In}_{0.75}\text{Al}_{0.25}\text{As}$  spacer separates the well from a Si -doping layer ( $N_{\text{Si}} = 1.3 \times 10^{12} \text{ cm}^{-2}$ ) placed above. At 4.2 K the electron mobility is  $1.1 \times 10^5 \text{ cm}^2\text{V}^{-1}\text{s}^{-1}$ , and the carrier density  $9.4 \times 10^{11} \text{ cm}^{-2}$ , as estimated from Shubnikov-de Haas measurements on a 60- $\mu\text{m}$ -wide Hall bar patterned on the same heterostructure of the devices presented here. From the mobility and density we deduced the momentum relaxation length  $l_m = 1.76 \mu\text{m}$ . The ballistic thermal length is  $l_T = \hbar v_F / \pi k_B T = 0.46 \mu\text{m}$  at 4.2 K, where  $v_F$  is the Fermi velocity and  $T$  is the temperature. The first fabrication step consisted in the deposition and annealing of Ni/AuGe/Ni/Au contacts. A Ti mask was then defined on the substrate surface by electron beam lithography, thermal evaporation of Ti, and lift-off. A reactive ion etching process was performed to transfer the geometry of the Ti mask on the semiconductor. The gas mixture employed for the dry etching was Ar/CH<sub>4</sub>/H<sub>2</sub>. The Ti mask was finally removed by wet chemical etching. Tens of devices were fabricated on the same sample showing highly-reproducible structural and transport properties. This was extremely useful towards the optimization of devices shape, and, in principle, could be used for tuning circuits parameters.

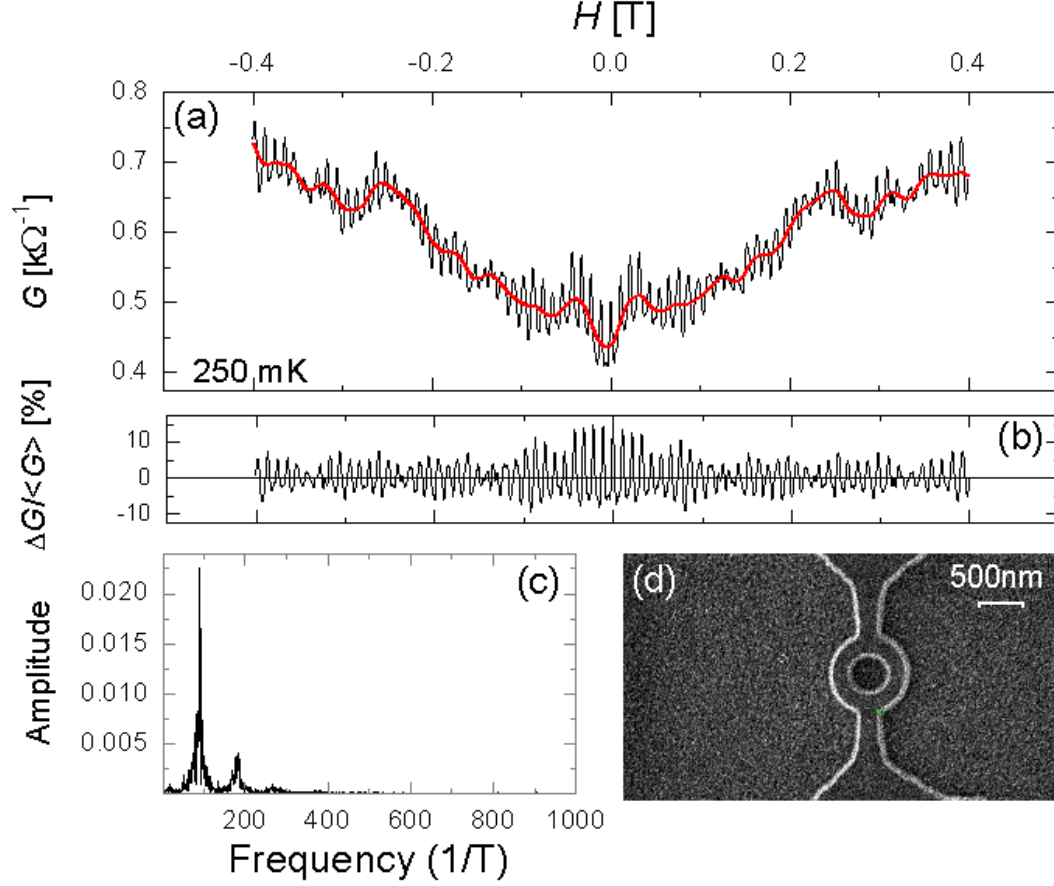


Fig. 1. (a) AB magnetic field conductance oscillation for a 350-nm-mean-radius ring shown in panel (d). (b)  $G(H)$  curve of panel (a) where the slowly-varying part (thick line) was subtracted. The peak to peak conductance oscillation amplitude is around the 20% of the average conductance value.

### 3 Coherent transport in $\text{In}_{0.75}\text{Ga}_{0.25}\text{As}$ -based nanostructures

Two-probe differential conductance measurements were performed with standard lock-in technique at 17.4 Hz. While measuring at 4.2 K or higher temperatures, the bias amplitude was kept at  $100 \mu\text{V}$ , while at 250 mK we used  $20 \mu\text{V}$ . Figure 1 shows the results for a 350 nm average radius ring. The conductance  $G$  exhibits AB modulations at 250 mK with a contrast  $\Delta G/G = 20\%$ , a remarkably high value for a structure defined using dry etching. This fact joined with the visibility of higher harmonics in  $G(H)$ 's Fast Fourier Transform (FFT) (see Fig. 1(c)), indicates that our process has a small impact on the structural and transport properties of the patterned nanostructures. The sample electric stability at 250 mK was tested on a time scale of the order of 15 hours. The two-probe conductance  $G(B)$  is expected to be symmetric with respect to the magnetic field. The high symmetry observed in magnetic field further confirms a good stability of the device. From the frequency value of the first harmonic peak we deduced an effective radius consistent with

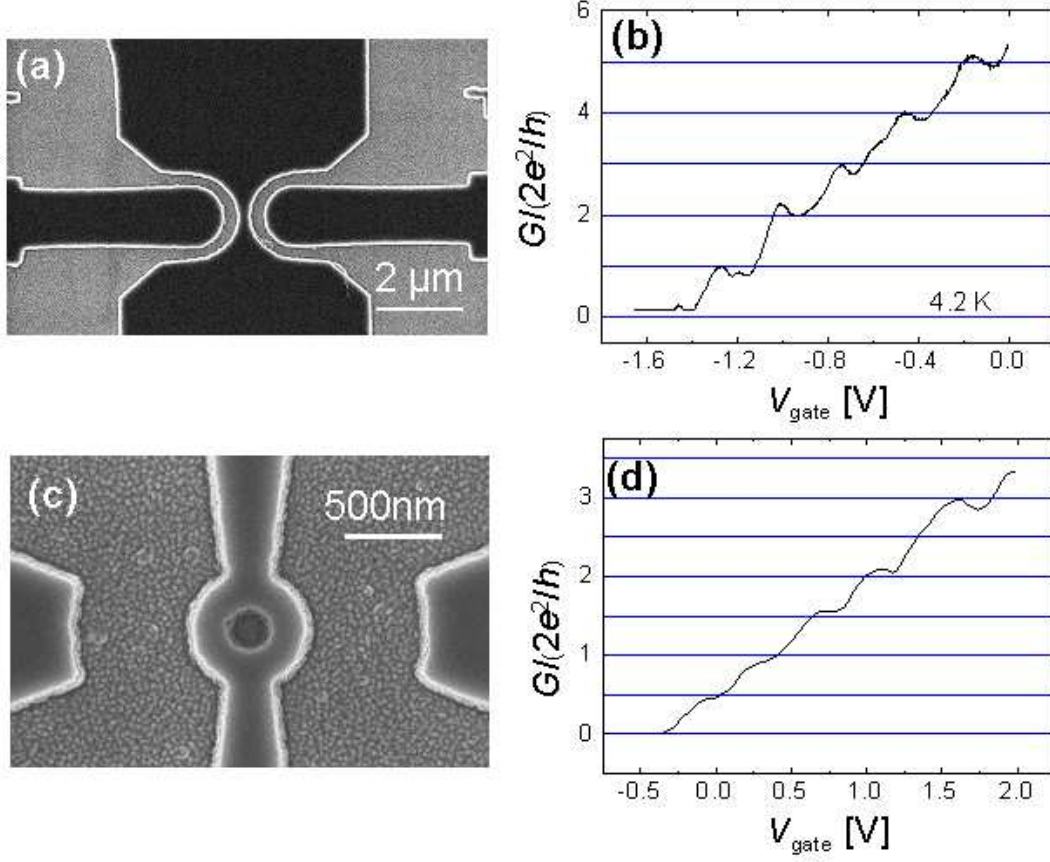


Fig. 2. (a) SEM micrograph of a 750-nm-radius and 200-nm-width QPC. (b) Conductance quantization as a function of voltage applied at both side gates of the QPC shown in (a). (c) SEM image of a ring featuring 200 nm mean radius and 120 nm arm width. Side gates are defined at a distance of 550 nm apart from each branch. (d) Zero-bias differential conductance at 4.2 K for the ring shown in (c).

the lithographically-defined average radius. All the rings tested confirmed the same behavior.

The strong and sharp lateral confinement provided by the etched side-walls and the reduced arms line-width lead to a large separation between energy sub-bands. This, joined with reduced electronic paths, allowed us to prove coherent transport in a 200-nm-radius ring similar to that of Fig. 2(c) up to  $T = 10$  K.

#### 4 Electric gating on $\text{In}_{0.75}\text{Ga}_{0.25}\text{As}$

The absence of the Schottky barrier makes it difficult to realize electrostatic gating on  $\text{In}_{0.75}\text{Ga}_{0.25}\text{As}$ -based nanostructures. We defined in-plane side gates patterned onto the 2DES itself. In Fig. 2(a) is shown a quantum point contact

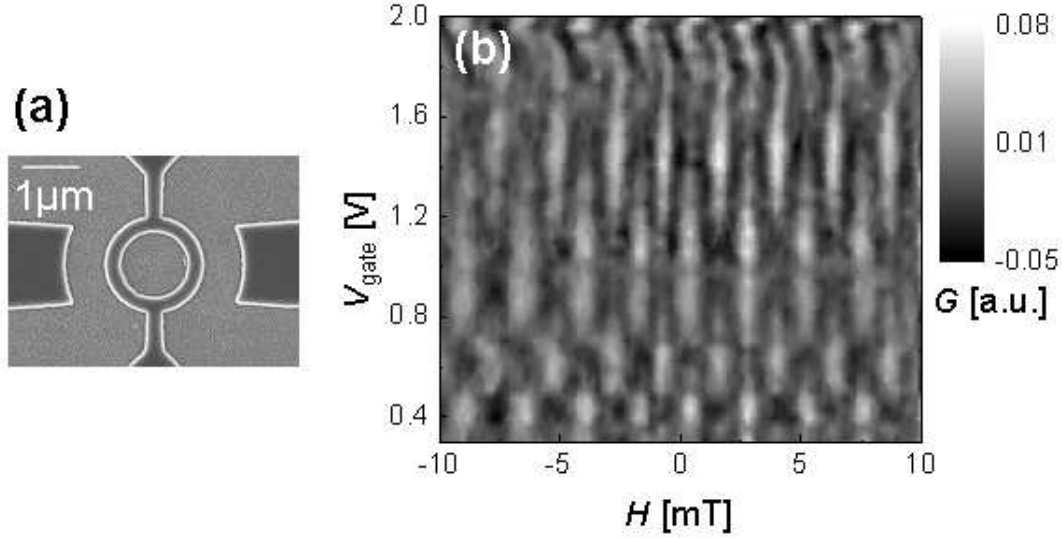


Fig. 3. (a) SEM micrograph of a 750-nm-radius ring featuring arm width of 200 nm. (b) Density plot of the conductance vs magnetic field ( $x$  axis) and voltage applied at one of the two gates ( $y$  axis). The other gate was biased at 1 V. The ac bias was set at  $20 \mu$  V and temperature at 280 mK.

(QPC). Five conductance steps are clearly visible at 4.2 K (see Fig. 2(b)). The pinch-off was induced by applying -1.6 V to the gates. At  $V = 0$  five transverse modes are present in the QPC.

Figure 2(c) displays the SEM micrograph of a typical 200-nm-radius ring, while Fig. 2(d) shows its differential conductance vs gate voltage. By applying a voltage sweep at both side gates the conductance exhibits well-defined steps corresponding to multiples of  $e^2/h$  (Fig. 2(d)). This can be explained considering two series quantum point contact at the entrance and at the exit of the ring. The same behavior have been observed also in GaAs/AlGaAs-based rings [9].

## 5 Voltage-controlled interferometers

Many theoretical [10,11,12] and experimental [13] works focused on the possibility to control devices conductance acting electrostatically on the quantum phase of charge carriers. In such systems it is not necessary to modify the charge density itself, like in conventional field-effect transistors, and this should result in higher switching speed and extended frequency range. Furthermore, phase-controlled devices could be fruitfully employed in complex coherent circuits, where phase manipulation is exploited for complex operations rather than the more simple control of conductance. One relevant geometry that allows the implementation of electrostatically-controlled interferometers is represented by a 2DEG ring where one of the two arms is capacitively-

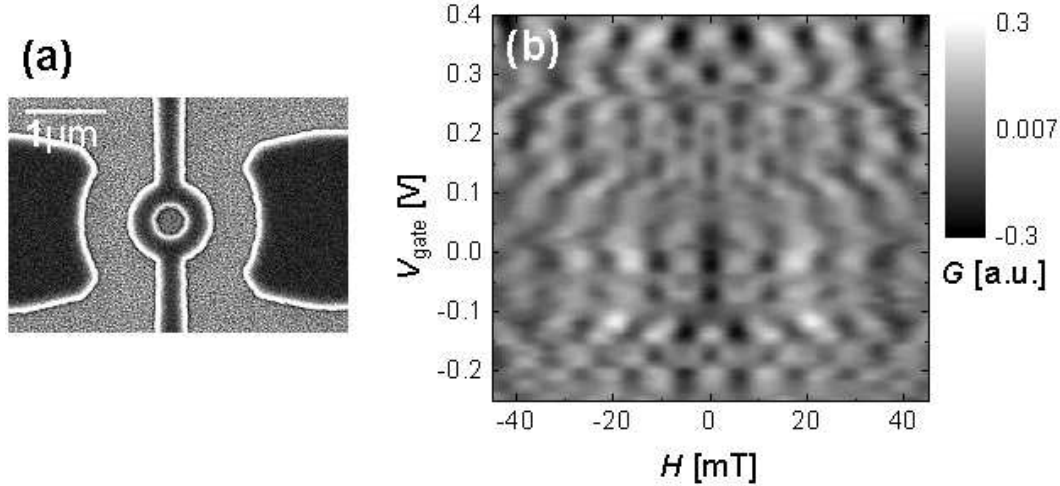


Fig. 4. (a) SEM image of a 350-nm-radius ring featuring arm width of 200 nm. (b) Density plot of the ring conductance like in Fig. 3(b).

coupled to a nearby gate [15,14]. Using the previously described process we fabricated rings of different sizes with gates like those shown in Figs. 2 to 4. By applying a bias to one of the gates while keeping the other at a fixed voltage it is possible to change the phase acquired by an electron traversing the arm closer to the former gate [11,12]. The effect of this extra-phase can be detected by analyzing the conductance vs magnetic field and gate voltage [14]. Figure 3 shows the SEM micrograph of a 750 nm ring and the density plot of its conductance at 280 mK as a function of the voltage applied at one side gate (vertical axis) and of the external magnetic field (horizontal axis). By changing the voltage at the side gate, the sequence of maxima and minima in magnetic field (bright and dark regions, respectively) are shifted by a half period  $h/2e$ . This shift occurs several times in the considered voltage range. Figure 4 shows the conductance density plot of a 350-nm-radius ring. In this case, due to the different gates geometry and to the reduced device size, the bias influences both the leads and the farthest arm of the ring, resulting in an irregular and distorted pattern. Density plots of Fig. 3 and Fig. 4 were obtained by subtracting the slowly-varying part of the conductance in order to evidence the oscillations in magnetic and electric field.

## 6 Conclusion

We demonstrated a highly-reproducible process based on  $\text{In}_{0.75}\text{Ga}_{0.25}\text{As}$  2DES, compliant with large scale integration and capable to reliably produce rings with average radius as small as 200 nm. The electric gating implemented with such a process efficiently controls charge density as well as induces conductance quantization. Voltage-controlled electron interferometers were demonstrated for different device size and geometries.

## References

- [1] F. Capotondi, G. Biasiol, D. Ercolani, V. Grillo, E. Carlino, F. Romanato, and L. Sorba, *Thin Solid Films* **484**, 400 (2005).
- [2] W. Desrat, F. Giazotto, V. Pellegrini, F. Beltram, F. Capotondi, G. Biasiol, L. Sorba, and D. K. Maude, *Phys. Rev. B* **69**, 245324 (2004).
- [3] W. Desrat, F. Giazotto, V. Pellegrini, M. Governale, F. Beltram, F. Capotondi, G. Biasiol, and L. Sorba, *Phys. Rev. B* **71**, 153314 (2005).
- [4] J. Nitta, T. Akazaki, H. Takayanagi, and T. Enoki, *Phys. Rev. Lett.* **78**, 1335 (1997).
- [5] Th. Schäpers, A. Kaluza, K. Neurohr, J. Malindretos, G. Crecelius, A. van der Hart, H. Hardtdegen, and H. Lüth, *Appl. Phys. Lett.* **71**, 3575 (1997).
- [6] A. Fuhrer, S. Lüscher, T. Ihn, T. Heinzel, K. Ensslin, W. Wegscheider, and M. Bichler, *Nature* **413**, 822 (2001).
- [7] D. Ferry and S. M. Goodnick, *Transport in Nanostructures* (Cambridge University Press, Cambridge, 1997).
- [8] K. Kajiyama, Y. Mizushima, and S. Sakata, *Appl. Phys. Lett.* **23**, 458 (1973).
- [9] S. Pedersen, A. E. Hansen, A. Kristensen, C. B. Sørensen, and P. E. Lindelof, *Phys. Rev. B* **61**, 5457 (2000).
- [10] F. Sols, M. Macucci, U. Ravaioli, and K. Hess, *Appl. Phys. Lett.* **54**, 350 (1989).
- [11] M. Cahay, S. Bandyopadhyay, and H. L. Grubin, *Phys. Rev. B* **39**, 12989 (1989).
- [12] D. Takai and K. Ohta, *Phys. Rev. B* **48**, 1537 (1993).
- [13] J. Appenzeller, Ch. Schroer, Th. Schäpers, A. v. d. Hart, A. Förster, B. Lengeler, and H. Lüth, *Phys. Rev. B* **53**, 9959 (1996).
- [14] B. Krafft, A. Förster, A. van der Hart, Th. Schäpers, *Physica E* **9**, 635 (2001); G. Cernicchiaro, T. Martin, K. Hasselbach, D. Mailly, and A. Benoit, *Phys. Rev. Lett.* **79**, 273 (1997).
- [15] E. B. Olshanetsky, *et al.*, *Physica E* **6**, 322 (2000); P. G. N. de Vegvar, G. Timp, P. M. Mankiewich, R. Behringer, and J. Cunningham, *Phys. Rev. B* **40**, 3491 (1989).